Available online at www.sciencedirect.com
SCIENCE DIRECT®
Biochemical and Biophysical Research Communications 328 (2005) 20–26
BBRC
www.elsevier.com/locate/ybbrc

Membrane topology of the electrogenic aspartate–alanine antiporter AspT of *Tetragenococcus halophilus*

Kei Nanatani[a], Fumito Ohonishi[a], Hiroshi Yoneyama[b], Tasuku Nakajima[a], Keietsu Abe[a,*]

[a] *Laboratory of Enzymology, Department of Molecular and Cell Biology, Graduate School of Agricultural Science, Tohoku University, Sendai 981-8555, Japan*

[b] *Laboratory of Animal Microbiology, Department of Microbial Biotechnology, Graduate School of Agricultural Science, Tohoku University, Sendai 981-8555, Japan*

Received 19 December 2004
Available online 1 January 2005

Abstract

AspT is an electrogenic aspartate:alanine exchange protein that represents the vectorial component of a proton-motive metabolic cycle found in some strains of *Tetragenococcus halophilus*. AspT is the sole member of a new family, the Aspartate:Alanine Exchanger (AAE) family, in secondary transporters, according to the computational classification proposed by Saier et al. (http://www.biology.ucsd.edu/~msaier/transport/). We analyzed the topology of AspT biochemically, by using fusion methods in combination with alkaline phosphatase or β-lactamase. These results suggested that AspT has a unique topology; 8 TMS, a large cytoplasmic loop (183 amino acids) between TMS5 and TMS6, and N- and C-termini that both face the periplasm. These results demonstrated a unique 2D-structure of AspT as the novel AAE family.

Keywords: Membrane topology; Aspartate:Alanine Antiporter; Proton-motive force; Fusion methods; Electrogenic

Some strains of *Tetragenococcus halophilus* (previously celled *T. halophila*) catalyze decarboxylation of L-aspartate with near-stoichiometric release of L-alanine and CO_2 [1,2]. L-aspartate decarboxylation is thought to be advantageous to the bacterial cells, because L-aspartate consumption concomitant with release of L-alanine generates, rather than consumes, metabolic energy and regulates the intracellular pH [3]. The net charge movement during the exchange of L-aspartate with L-alanine results in a membrane potential of physiological polarity. Furthermore, decarboxylation reactions consume scalar protons, and thus generate a pH gradient of physiological polarity. The combined activities of the precursor–product exchange and decarboxylation result in a proton-motive force (PMF) that is sufficiently high to drive ATP synthesis via the bacterial F_0F_1 ATPase. Such metabolic systems are proposed as a proton-motive metabolic cycle, and the prototype model is found in *Oxalobacter formigenes* [4–6]. Over the past 10 years, a number of presumed proton-motive metabolic decarboxylation cycles have been identified in several bacterial species, including glutamate to γ-aminobutyrate [7–9], malate to lactate [10], and histidine to histamine [11].

In one strain, *T. halophilus* D10, we previously found a 25-kb plasmid responsible for the trait of L-aspartate decarboxylation [1], and cloned and sequenced the *asp* operon, which consists of two genes that we designated *aspD* and *aspT*. *aspD* encodes an L-aspartate β-decarboxylase (AspD), and *aspT* an aspartate:alanine antiporter (AspT) [3]. The two genes were successfully expressed in *Escherichia coli*. We solubilized AspT from

* Corresponding author. Fax: +81 22 717 8778.
E-mail address: kabe@biochem.tohoku.ac.jp (K. Abe).

0006-291X/$ - see front matter © 2004 Elsevier Inc. All rights reserved.
doi:10.1016/j.bbrc.2004.12.133

membranes of the *E. coli* cells and demonstrated the electrogenic character of the aspartate:alanine exchange catalyzed by AspT using proteoliposomes [3].

Analysis of the amino acid sequence of AspT revealed it to be a hydrophobic membrane protein. The biochemical features of AspT transport demonstrated by using proteoliposomes indicated that AspT should be classified as a conventional secondary transport protein, as an electrogenic antiporter similar to the prototype of precursor–product exchanger OxlT from *O. formigenes* [4–6,12,13]. However, AspT had low sequence similarities (<20%) of amino acids to known membrane transporters, including PMF-generating antiporters [4,8,14], suggesting that the structures of PMF generating antiporters are divergent. At this time, *T. halophilus* AspT is the sole transporter that has been biochemically shown to be an electrogenic aspartate:alanine exchanger, and it is the sole member of a family of secondary transporters called the Aspartate:Alanine Exchanger (AAE) family according to the computational classification proposed by Saier (http://www.biology.ucsd.edu/~msaier/transport/). However, the secondary structure of AspT has remained unclear. Prediction of the AspT membrane topology from hydropathy profiles by using several prediction programs gave several different models having 9–12 transmembrane segments (TMS), and the segments having middle range of hydrophobicity were ambiguously predicted in the present study. The topology of cytoplasmic membrane proteins in bacteria has often been studied biochemically by using *phoA* and *blaM* gene-fusion methods [15–17]. Both alkaline phosphatase (PhoA) and β-lactamase (BlaM) are enzymatically active after translocation to the periplasm, but are inactive when localized in the cytoplasm [15,16]. Therefore, we biochemically analyzed the membrane topology of AspT by fusion methods, using PhoA and BlaM as reporter proteins.

Materials and methods

Bacterial strains and plasmids. The *E. coli* strains used were, first, LMG194 [F$^-$ Δ*ara*714 *leu*::Tn10 Δ*lacX*74 Δ*phoA* (*Pvu*II) *galE galK thirpsL*] [18], which was used for expression of the aspartate:alanine antiporter (AspT)–alkaline phosphatase (PhoA) fusion proteins by means of the pBAD*phoA* plasmid. pBAD*phoA* is a cloning vector containing a signal-sequenceless *phoA* with a *Kpn*I and a *Nco*I cloning site just upstream of *phoA*. The construction of pBAD*phoA* from pSWFII [19] and pBAD22 [18] will be described elsewhere. Second, *E. coli* strain XL1 blue (*recA*1, *endA*1, *gyrA*96, *thi*, *hsdR*17, *supE*44, *relA*1, *lac* [F′, *proAB*, *lacI*^{q}ZΔ*M*15, Tn10 (Tet^r)]) harboring pMS421 (Spec^r, LacI^q) is here called strain XL3 [4] and was used for expression of the AspT–BlaM fusion proteins by means of the expression vector pYZ4 containing Kan^r as a selection marker [17]. pKM1 is the mature β-lactamase (BlaM) cassette plasmid, Tet^r [20].

Hydropathy analyses of AspT. The hydropathy profile of the *T. halophilus* AspT was derived by the method of Eisenberg [21] using a sliding window of 15 amino acids (Fig. 1).

Analysis of AspT–PhoA, AspT–BlaM fusion proteins. We biochemically investigated the two-dimensional membrane topology of AspT by using PhoA and BlaM fusion methods. The compartmental nature of PhoA and BlaM has been well established, and they are routinely used to investigate the topology of integral membrane proteins [22,23]. Deletion derivatives of AspT were amplified from plasmid pBluscript II KS (+) including the *aspT* gene by PCR using primers that generated unique restriction sites at the 5′ (*Nco*I) and 3′ (*Kpn*I) ends. The 3′ sites were designed to create in-frame fusions to the reporter cassettes upon ligation into either pBAD-PhoA (*phoA*) or pYZ4 (*blaM*). Such 18 fusions were constructed and sequenced to verify the fusion junctions. Alkaline phosphatase specific activities of the AspT–PhoA chimeras were determined as described by Guan et al. [22]. The MICs of carbenicillin for strains expressing AspT–BlaM fusions were determined by spotting 5 μl of a 10-3 dilution of an overnight culture onto Luria–Bertani agar plates containing the antibiotic. The plates were incubated at 30 °C for 24 h. The concentrations of carbenicillin ranged from 0 to 800 μg/ml.

SDS–PAGE and Western blotting. Whole-cell lysates were prepared and subjected to polyacrylamide (10% or 12.5%) gel electrophoresis in the presence of SDS. After electrophoresis, the proteins were transferred to a polyvinylidene difluoride (PVDF) membrane (Nippon Genetics, Tokyo, Japan) by semidry electrophoretic blotting. PhoA and BlaM fusion proteins were detected with a PhoA detection kit (Bio-Rad Laboratories, Hercules, CA) according to the manufacturer's

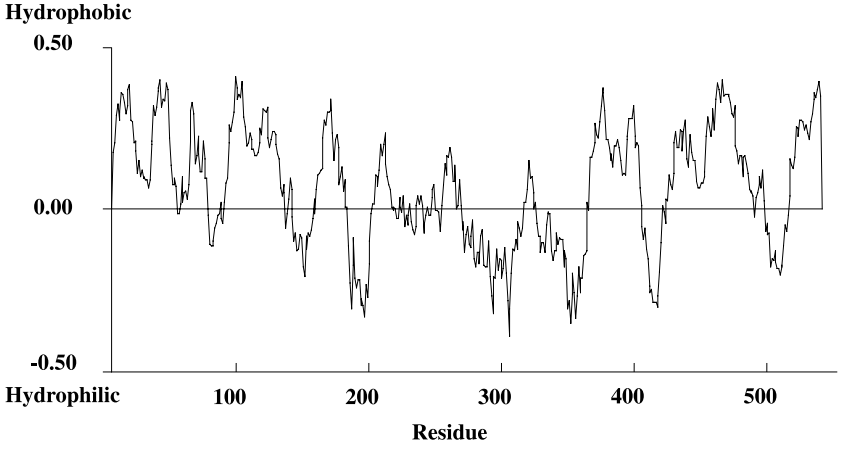

Fig. 1. Hydropathy analysis of *T. halophilus* AspT. The hydropathy plot was calculated with the algorithm of Eisenberg [21] using a window size of 15 residues.

instructions. Antisera were used at following dilutions: anti-bacterial alkaline phosphatase mouse monoclonal antibodies (Sigma Chemical, Tokyo, Japan), 1:7500; anti-mouse immunoglobulin G (heavy and light chains) horse polyclonal antibody PhoA-conjugate (Vector Laboratories, Burlingame, CA), 1:7500; anti-bacterial β-lactamase rabbit polyclonal antibodies (5′–3′, Boulder, CO), 1:1000; and anti-rabbit immunoglobulin G (heavy and light chains) goat polyclonal antibody PhoA-conjugate (Nacalai Tesque, Kyoto, Japan), 1:5000.

Results and discussion

Hydropathy analyses of AspT

Despite the fact that the accumulating number of bacterial genome sequences reveals that AspT homologs may be present in several bacterial species, the structure of AspT remains unknown. The hydropathy profile of the *T. halophilus* AspT (Fig. 1) suggests that AspT is a polytopic membrane protein. Further analyses of AspT hydropathy by using the programs the SOSui (http://sosui.proteome.bio.tuat.ac.jp/sosuiframe0.html, [24]), TMHMM (http://www.cbs.dtu.dk/services/TMHMM-2.0/, [25,26]), and TMPred (http://www.ch.embnet.org/software/TMPRED_form.html, [27]) predicted the presence of 9–12 transmembrane segments (TMS) in AspT, resulting in ambiguity and discrepancy of TMS predictions among the three models.

Analysis of AspT–PhoA fusion proteins

We biochemically investigated the two-dimensional membrane topology of AspT by using PhoA and BlaM fusion methods. The locations of these fusions along with their enzymatic activities and subcellular locations are indicated in Table 1. Expression of the hybrid proteins derived from pBAD*phoA* is under the control of the *araBAD* promoter; therefore, cells harboring the fusions were induced in the presence of 0.4% L-arabinose. To ascertain the proper expression of the hybrid proteins in the *E. coli* host (LMG194), cells were resuspended to 4 μg protein/μl in loading buffer and incubated for 12 h at 37 °C, after which 15 μl samples were loaded onto sodium dodecyl sulfate (SDS)–polyacrylamide gels containing 10% polyacrylamide. After electrophoresis, the proteins were transferred to a polyvinylidene difluoride (PVDF) membrane (Nippon Genetics, Tokyo, Japan) by semidry electrophoretic blotting, and visualized by immunoblotting using anti-bacterial alkaline phosphatase mouse monoclonal antibodies (Fig. 2A). The mobility of most of the fusion proteins was within the range appropriate to their expected molecular mass. Some fusion proteins yielded extra bands having lower molecular mass than expected, suggesting proteolysis. In particular, more extra bands were observed for hybrid proteins in which the fusion junctions were likely to face the periplasmic side of the membrane (Cys^{476}, Ser^{543}). Expression levels of some fusion proteins were very low (Lys^{87}, Ala^{126}, Lue^{151}, Ala^{198}, Ser^{448}, Ser^{452}, and Glu^{506}), but we could confirm their expression by loading a larger amount of proteins (120 μg) onto SDS–polyacrylamide gels (data not shown). Hybrid proteins with junction sites located after Gly^{62}, Ala^{126}, Leu^{151}, Ser^{386}, Lys^{411}, Ser^{448}, Ser^{452}, Cys^{476}, and Ser^{543} of AspT showed high alkaline phosphatase activities, indicating localization of these sites at or close to the periplasmic side of the membrane. The results for AspT–PhoA hybrid proteins fused at Ser^{543} indicate that the C-terminal amino acids of the corresponding AspT fragments are located at, or close to, the periplasmic side of the membrane. Low alkaline phosphatase activities were observed when the fusion sites were located after Ser^{33}, Lys^{87}, Ala^{198}, Ala^{273}, Glu^{348}, and Glu^{506} of AspT. The PhoA-fusion analysis of AspT suggested that AspT has 8 TMS, and a large cytoplasmic loop (183 amino acids) located between TMS5 and TMS6. Both the N- and C-termini appear to face the periplasm.

Table 1
Characteristics of AspT chimeric proteins

Amino acid residue of fusion postion[a]	Activity of PhoA (10^{-3} units/OD_{650})[b]	MIC (μg/ml)[c] of carbenicillin	Localization[d]
N-AspT (half)		100	Out
N-AspT (full-length)		<50	N.D.[e]
Ser^{33}	3.65	<50	In
Gly^{62}	14.1	>800	Out
Lys^{87}	3.26	<50	In
Ala^{126}	34.6	>800	Out
Leu^{151}	20.7	800	Out
Ala^{198}	5.10	<50	In
Ala^{273}	5.71	<50	In
Glu^{348}	3.97	<50	In
Ser^{366}	7.00	<50	In
Ser^{386}	327	>800	Out
Lys^{411}	86.6	>800	Out
Gin^{427}	8.73	800	M or Out
Ala^{436}	4.35	400	M or Out
Ser^{448}	146	800	Out
Ser^{452}	40.0	200	Out
Cys^{476}	55.7	200	Out
Glu^{506}	3.16	<50	In
Ser^{543}	103	400	Out

[a] Last amino acid residue of AspT before the fusion point.
[b] Alkaline phosphatase activity was measured in exponentially growing suspension cultures.
[c] Carbenicillin resistance of *E. coli* XL3 cells expressing AspT–BlaM fusion proteins was measured as the single-cell minimum inhibitory concentration (MIC).
[d] Location as deter-mined by alkaline phosphatase specific activity and the MIC values: Out, periplasmic; In, cytoplasmic; TM, transmembrane region; and M, membrane.
[e] Since expression of the signal-less BlaM fused at its C-terminus with full-length AspT was low, this BlaM-full-length AspT fusion had a low MIC in the presence of carbenicillin.

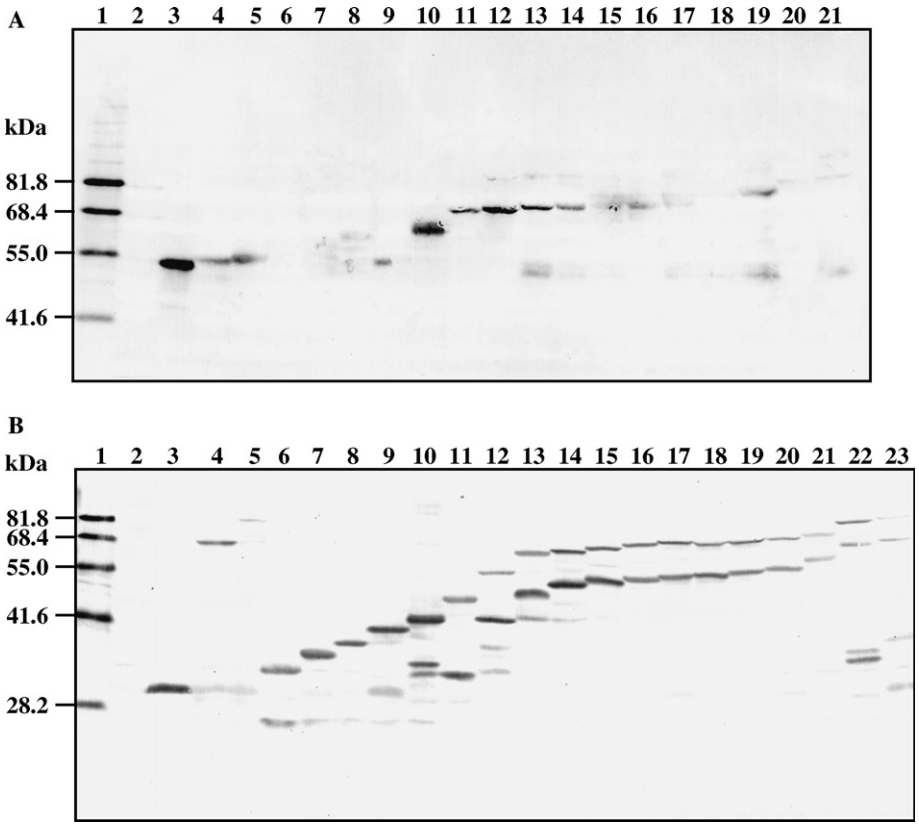

Fig. 2. Western blot analysis of AspT–PhoA fusion proteins expressed in *E. coli* LMG194 (A) and AspT–BlaM fusion proteins expressed in *E. coli* XL-3 (B). Whole-cell lysates were prepared, subjected to polyacrylamide (10% or 12.5%) gel electrophoresis in the presence of SDS, electroblotted onto a polyvinylidene difluoride membrane, and visualized with monoclonal antibodies against alkaline phosphatase (A) or polyclonal antibodies against β-lactamase (B). The samples are coded here according to the fusion site (e.g., Ser^{33} indicates residues 1–33 of AspT fused with PhoA). (A) Lane 1, molecular weight markers (Western doctor); lane 2, no plasmid; lane 3, pBAD*phoA* ; lane 4, C-Ser^{33}; lane 5, C-Gly^{62}; lane 6, C-Lys^{87}; lane 7, C-Ala^{126}; lane 8, C-Lue^{151}; lane 9, C-Ala^{198}; lane 10, C-Ala^{273}; lane 11, C-Glu^{348}; lane 12, C-Ser^{366}; lane 13, C-Ser^{386}; lane 14, C-Lys^{411}; lane 15, C-Gln^{427}; lane 16, C-Ala^{436}; lane 17, C-Ser^{448}; lane 18, C-Ser^{452}; lane 19, C-Cys^{476}; lane 20, C-Glu^{506}; and lane 21, C-Ser^{543}. (B) Lane 1, molecular weight markers (Western doctor); Lane 2, pYZ4; Lane 3, BlaM; lane 4, N-AspT (half); lane 5, N-AspT (full-length); lane 6, C-Ser^{33}; lane 7, C-Gly^{62}; lane 8, C-Lys^{87}; lane 9, C-Ala^{126}; lane 10, C-Lue^{151}; lane 11, C-Ala^{198}; lane 12, C-Ala^{273}; lane 13, C-Glu^{348}; lane 14, C-Ser^{366}; lane 15, C-Ser^{386}; lane 16, C-Lys^{411}; lane 17, C-Gln^{427}; lane 18, C-Ala^{436}; lane 19, C-Ser^{448}; lane 20, C-Ser^{452}; lane 21, C-Cys^{476}; lane 22, C-Glu^{506}; and lane 23, C-Ser^{543}.

Analysis of AspT–BlaM fusion proteins

Since AspT–PhoA fusion analysis suggested the unique structural features of AspT as described above, we further examined the implications of the AspT–PhoA fusion results by using BlaM–AspT fusions for N-terminal analysis and AspT–BlaM fusions for analyzing other junction positions with the C-terminus of AspT. We designed two BlaM–AspT fusion genes; one expressed β-lactamase lacking its signal sequence fused at its C-terminus with the full-length of AspT, and the other expressed the same protein fused with the N-terminal half of AspT. We also obtained 18 independent fusion genes expressing a C-terminal deletion series of AspT fused with BlaM at the C-termini of the truncated AspTs. The expression of hybrid proteins derived from pYZ4 *blaM–aspT* or pYZ4 *aspT–blaM* is under the control of the *lacUV5* promoter; therefore, cells harboring the fusions were induced in the presence of IPTG. To examine proper expression of the hybrid proteins in the *E. coli* host (XL3), we ran SDS–PAGE of extracts prepared from whole cells harboring the plasmids and visualized the protein by immunoblotting using anti-bacterial β-lactamase rabbit polyclonal antibodies. The results of Fig. 2B show that the hybrid proteins from Ser^{33} through Ser^{543} lined up according to increasing molecular mass as the fusion sites became closer to the C-terminal end of the full-length protein. Expression of the signal-less BlaM fused at its C-terminus with the N-terminal half of AspT (Fig. 2B, lane 4) was observed; however, expression of BlaM fused at the C-terminus with the full-length of AspT was significantly low (Fig. 2B, lane 5). Signal-less BlaM fused at its C-terminus with the N-terminal half of AspT, and AspT–BlaM hybrid proteins with fusion locations at Gly^{62}, Ala^{126}, Leu^{151}, Ser^{386}, Lys^{411}, Gln^{427}, Ala^{436}, Ser^{448}, Ser^{452}, Cys^{476}, and the C-terminal end Ser^{543} of AspT showed carbenicillin resistance (100–800 μg/ml), suggesting that the fusion sites including both N- and C-termini face the periplasm. Since expression of signal-less BlaM fused

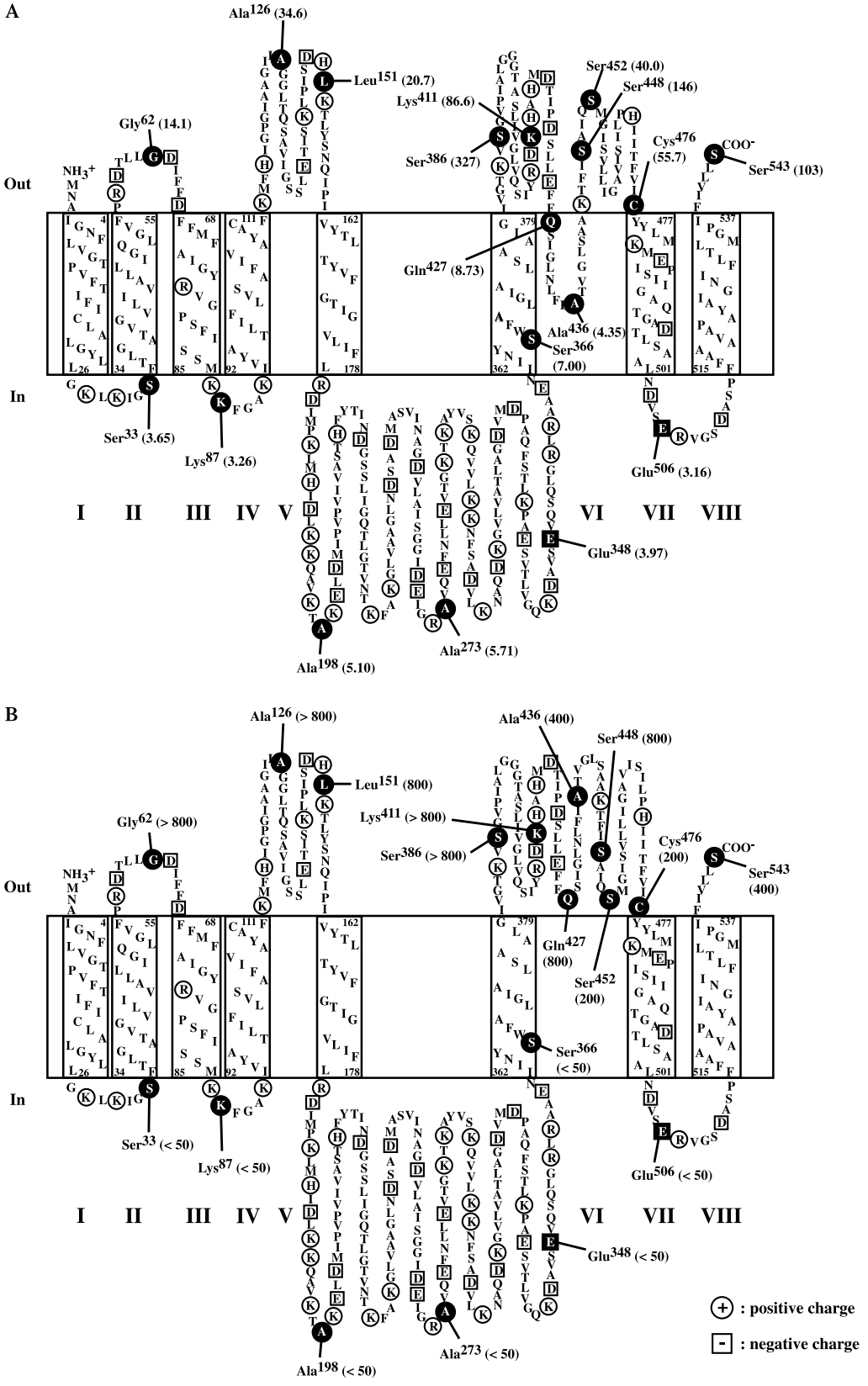

Fig. 3. Topological model of AspT, based on the results of PhoA fusions (A) and BlaM fusions (B). (A) PhoA fusion sites are indicated by black circles. The numbers in parentheses indicate unit of PhoA activity (units). (B) BlaM fusion sites are indicated by black circles. The numbers in parentheses correspond to the MIC (μg/ml) of β-lactamase. Positively charged residues and negatively charged residues are indicated by open circles and open boxes, respectively.

with the full-length of AspT was significantly low, the low expression levels would be responsible for the carbenicillin sensitivity of cells expressing this fusion. Thus, we excluded this fusion from our predictions. On the contrary, the remaining fusions with junction sites at Ser^{33}, Lys^{87}, Ala^{198}, Ala^{273}, Glu^{348}, Ser^{366}, and Glu^{506} were sensitive to carbenicillin at concentrations <50 μg/ml, indicating that these fusion sites are most likely located on the cytoplasmic side of the membrane. Thus, the results obtained with BlaM fusions are in good agreement with those obtained with AspT–PhoA hybrid proteins (Table 1).

To our knowledge, transporters in which both the N- and C-termini are localized toward the periplasm are scarcely reported. Although we had constructed 6× histidine-tag fusions at the N and C -termini of AspT prior to the PhoA and BlaM fusion experiments reported here, we did not succeed in expressing the two histidine-tag fusions (data not shown). Since the N- and C-termini of the full-length of AspT face the periplasmic side according to the results of the PhoA and BlaM fusion analyses, positive charges in 6× histidine-tag might inhibit traversal of the two termini across the membrane and consequently be responsible for the failure in expression of the two terminal histidine-tag fusions.

The results of AspT–PhoA fusion analysis also indicated the possibility of a reentrant loop (Glu^{424}–Ser^{448}) that seems to be embedded in the cytoplasmic membrane from the outside between TMS6 and TMS7, for the following reasons. Cells expressing PhoA fused with AspT at Glu^{424} (data not shown) and Ser^{448} obviously had alkaline phosphatase activity, suggesting a periplasmic localization of these two sites. However, cells expressing PhoA fused at Gln^{427} and Ala^{436} of AspT showed intermediate levels of alkaline phosphatase activity. The 23-amino acid-chain between Glu^{424} and Ser^{448} is not long enough to traverse the cytoplasmic membrane twice. Similar reentrant loops have been found in other transporters and channels, including synaptic glutamate transporter GLT-1 [28,29] and potassium channel KcsA [30]. However, since AspT–BlaM fusions joined at Gln^{427} and Ala^{436} of AspT showed carbenicillin resistance, the possibility that the region between Glu^{424} and Ser^{448} has periplasmic localization cannot be ruled out. Fusion methods that use reporter proteins having a larger molecular mass do not yet have enough resolution to analyze the location of this putative reentrant loop. In addition to the periplasmic localization of the two terminal ends of AspT, its large cytoplasmic loop consisting of 183 amino acid residues gives a characteristic feature to the two-dimensional structure of AspT among known secondary transporters whose membrane topologies have been biochemically analyzed or computationally predicted. To our knowledge, the large cytoplasmic loop of AspT is significantly longer than those observed in other secondary transporters such as CitS [31] and GltT [32]. We found 10 probable AspT-orthologous genes in recent bacterial genome information by using the tBlastn network service, and all of them are consistent with large cytoplasmic loops similar to that of Tetragenococcal AspT, according to the TMS prediction program SOSui (data not shown).

Our new topological model of AspT, based on the data shown in the present study (Fig. 3), represents a new class of secondary transporters, an AAE family previously predicted by Saier et al. (http://www.biology.ucsd.edu/~msaier/transport/) according to its amino acid sequence and hydropathy [3]. In addition, the results of helical wheel analysis (data not shown) tentatively suggested the presence of a positively charged residue (Arg^{76}) within TMS3 and charged Lys^{481}, Glu^{483}, and Asp^{495} residues in TMS7 (Fig. 3). The charged residues in the hydrophobic sectors imply that TMS3 and TMS7 form a part of the substrate translocation pathway.

Acknowledgment

We thank Dr. Taiji Nakae for the gift of plasmid pBAD*phoA* and *E. coli* LMG194.

References

[1] T. Higuchi, K. Uchida, K. Abe, Aspartate decarboxylation encoded on the plasmid in the soy sauce lactic acid bacterium, *Tetragenococcus halophila* D10, Biosci. Biotechnol. Biochem. 62 (1998) 1601–1603.

[2] K. Uchida, Trends in preparation and uses of fermented and acidhydrolyzed soy sauce, in: Proceedings of the World Congress on Vegetable Protein Utilization in Human Foods and Animal Feedstuffs, Kraft, Inc., 1988, pp. 78–83.

[3] K. Abe, F. Ohnishi, K. Yagi, T. Nakajima, T. Higuchi, M. Sano, M. Machida, R.I. Sarker, P.C. Maloney, Plasmid-encoded asp operon confers a proton motive metabolic cycle catalyzed by an aspartate-alanine exchange reaction, J. Bacteriol. 184 (2002) 2906–2913.

[4] K. Abe, Z.S. Ruan, P.C. Maloney, Cloning, sequencing, and expression in *Escherichia coli* of OxlT, the oxalate:formate exchange protein of Oxalobacter formigenes, J. Biol. Chem. 271 (1996) 6789–6793.

[5] V. Anantharam, M.J. Allison, P.C. Maloney, Oxalate:formate exchange. The basis for energy coupling in *Oxalobacter*, J. Biol. Chem. 264 (1989) 7244–7250.

[6] P.C. Maloney, R.T. Yan, K. Abe, Bacterial anion exchange: reductionist and integrative approaches to membrane biology, J. Exp. Biol. 196 (1994) 471–482.

[7] T. Higuchi, H. Hayashi, K. Abe, Exchange of glutamate and gamma-aminobutyrate in a *Lactobacillus* strain, J. Bacteriol. 179 (1997) 3362–3364.

[8] J.W. Sanders, K. Leenhouts, J. Burghoorn, J.R. Brands, G. Venema, J. Kok, A chloride-inducible acid resistance mechanism in *Lactococcus lactis* and its regulation, Mol. Microbiol. 27 (1998) 299–310.

[9] M.P. Castanie-Cornet, J.W. Forster, *Escherichia coli* acid resistance: cAMP receptor protein and a 20 bp *cis*-acting sequence control pH and stationary phase expression of the gadA and gadBC glutamate decarboxylase genes, Microbiology 147 (2001) 709–715.
[10] B. Poolman, D. Molenaar, E.J. Smid, T. Ubbink, T. Abee, P.P. Renault, W.N. Konings, Malolactic fermentation: electrogenic malate uptake and malate/lactate antiport generate metabolic energy, J. Bacteriol. 173 (1991) 6030–6037.
[11] D. Molenaar, J.S. Bosscher, B. ten Brink, A.J. Driessen, W.N. Konings, Generation of a proton motive force by histidine decarboxylation and electrogenic histidine/histamine antiport in *Lactobacillus buchneri*, J. Bacteriol. 175 (1993) 2864–2870.
[12] P.C. Maloney, Bacterial transporters, Curr. Opin. Cell Biol. 6 (1994) 571–582.
[13] P.C. Maloney, T.H. Wilson, Ion-coupled transport and transporters, in: F.C. Neidhardt, J.L. Ingraham, K.B. Low, B. Magasanik, M. Schaechter, H.D. Umbarger (Eds.), *Escherichia coli* and *Salmonella typhimurium*: Cellular and Molecular Biology, ASM Press, Washington, DC, 1996, pp. 1130–1148.
[14] C. Marty-Teysset, J.S. Lolkema, P. Schmitt, C. Divies, W.N. Konings, Membrane potential-generating transport of citrate and malate catalyzed by CitP of *Leuconostoc mesenteroides*, J. Biol. Chem. 270 (1995) 25370–25376.
[15] C. Manoil, J. Beckwith, TnphoA: a transposon probe for protein export signals, Proc. Natl. Acad. Sci. USA 82 (1985) 8129–8133.
[16] C. Manoil, J.J. Mekalanos, J. Beckwith, Alkaline phosphatase fusions: sensors of subcellular location, J. Bacteriol. 172 (1990) 515–518.
[17] Y.B. Zhang, J.K. Broome-Smith, Correct insertion of a simple eukaryotic plasma-membrane protein into the cytoplasmic membrane of *Escherichia coli*, Gene 96 (1990) 51–57.
[18] L.M. Guzman, D. Belin, M.J. Carson, J. Beckwith, Tight regulation, modulation, and high-level expression by vectors containing the arabinose PBAD promoter, J. Bacteriol. 177 (1995) 4121–4130.
[19] M. Ehrmann, D. Boyd, J. Beckwith, Genetic analysis of membrane protein topology by a sandwich gene fusion approach, Proc. Natl. Acad. Sci. USA 87 (1990) 7574–7578.
[20] J.K. Broome-Smith, M. Tadayyon, Y. Zhang, β-Lactamase as a probe of membrane protein assembly and protein transport, Mol. Microbiol. 4 (1990) 1637–1644.
[21] D. Eisenberg, E. Schwarz, M. Komaromy, R. Wall, Analysis of membrane and surface protein sequences with the hydrophobic moment plot, J. Mol. Biol. 179 (1984) 125–142.
[22] L. Guan, M. Ehrmann, H. Yoneyama, T. Nakae, Membrane topology of the xenobiotic-exporting subunit, MexB, of the MexA, B-OprM extrusion pump in *Pseudomonas aeruginosa*, J. Biol. Chem. 274 (1999) 10517–10522.
[23] C. Manoil, Analysis of membrane protein topology using alkaline phosphatase and beta-galactosidase gene fusions, Methods Cell Biol. 34 (1991) 61–75.
[24] T. Hirokawa, S. Boon-Chieng, S. Mitaku, SOSUI: classification and secondary structure prediction system for membrane proteins, Bioinformatics 14 (1998) 378–379.
[25] A. Krogh, B. Larsson, G. von Heijne, E.L. Sonnhammer, Predicting transmembrane protein topology with a hidden Markov model: application to complete genomes, J. Mol. Biol. 305 (2001) 567–580.
[26] E.L. Sonnhammer, G. von Heijne, A. Krogh, A hidden Markov model for predicting transmembrane helices in protein sequences, Proc. Int. Conf. Intell. Syst. Mol. Biol. 6 (1998) 175–182.
[27] K. Hofman, W. Stoffel, TMbase: a database of membrane spanning protein segments, Biol. Chem. Hoppe-Seyler 374 (1993) 166.
[28] L. Brocke, A. Bendahan, M. Grunewald, B.I. Kanner, Proximity of two oppositely oriented reentrant loops in the glutamate transporter GLT-1 identified by paired cysteine mutagenesis, J. Biol. Chem. 277 (2002) 3985–3992.
[29] M. Grunewald, A. Bendahan, B.I. Kanner, Biotinylation of single cysteine mutants of the glutamate transporter GLT-1 from rat brain reveals its unusual topology, Neuron 21 (1998) 623–632.
[30] D.A. Doyle, J.M. Cabral, R.A. Pfuetzner, A. Kuo, J.M. Gulbis, S.L. Cohen, B.T. Chait, R. Mackinnon, The structure of the potassium channel: molecular basis of K+ conduction and selectivity, Science 280 (1998) 69–77.
[31] M. van Geest, J.S. Lolkema, Membrane topology of the Na(+)/citrate transporter CitS of Klebsiella pneumoniae by insertion mutagenesis, Biochim. Biophys. Acta 1466 (2000) 328–338.
[32] D.J. Slotboom, W.N. Konings, J.S. Lolkema, Cysteine-scanning mutagenesis reveals a highly amphipathic, pore-lining membrane-spanning helix in the glutamate transporter GltT, J. Biol. Chem. 276 (2001) 10775–10781.